

## EFFECT OF Gd<sub>2</sub>O<sub>3</sub> DOPING ON DIELECTRIC PROPERTIES OF Ba(Zr<sub>0.1</sub>Ti<sub>0.9</sub>)O<sub>3</sub> CERAMICS

Z. LI<sup>a,b,\*</sup>, Y. LI<sup>c</sup>, H. TAN<sup>a,b</sup>, L. CI<sup>a,b</sup>

<sup>a</sup>Chemical College, Shijiazhuang University, Shijiazhuang 050035, China

<sup>b</sup>Hebei Building Ceramics Engineering Research Centre, Shijiazhuang 050035, China

<sup>c</sup>Analysis and Testing Research Centre, North China University of Science and Technology, Tangshan 063210, China)

Using BaCO<sub>3</sub>, TiO<sub>2</sub>, ZrO<sub>2</sub> and Gd<sub>2</sub>O<sub>3</sub> as the starting materials, the Ba(Zr<sub>0.1</sub>Ti<sub>0.9</sub>)O<sub>3</sub> ceramics are prepared using solid state synthesis method, and effects of Gd<sub>2</sub>O<sub>3</sub> dopant on microstructure and dielectric properties of Ba(Zr<sub>0.1</sub>Ti<sub>0.9</sub>)O<sub>3</sub> ceramics are investigated. The results show that the crystal structure for Ba(Zr<sub>0.1</sub>Ti<sub>0.9</sub>)O<sub>3</sub> ceramics is a single perovskite structure, and the doping of Gd<sup>3+</sup> does not generate new phase. With the Gd<sub>2</sub>O<sub>3</sub> concentration increasing, the grain size increases continuously, when the doping amount  $x \geq 0.5$  mol %, the grain size basically remains unchanged, the grain size is uniform. With the Gd<sub>2</sub>O<sub>3</sub> content increasing, the dielectric constants rose first and then decreased under different sintering conditions of 1280 °C, 1300 °C, 1330 °C, and 1350 °C. When the sintering temperature is 1350 °C and the Gd<sup>3+</sup> doping amount is  $x = 0.5$  mol %, the dielectric loss is minimal, the dielectric constant is the highest, and the dielectric performance at room temperature is optimal. Gd<sub>2</sub>O<sub>3</sub> doping has little effect on the movement of the Curie point of BZT ceramics, but the doping of Gd<sub>2</sub>O<sub>3</sub> can increase the peak of the dielectric peak at the Curie point.

(Received July 19, 2019; Accepted January 3, 2020)

*Keywords:* Ceramics, Dielectric properties, Dope, Microstructure

### 1. Introduction

Barium titanate (BT) ceramics can be widely used in multi-layer ceramic capacitors for its high dielectric constant, good ferroelectric properties [1-3]. Ceramic samples based on barium titanate are among the most studied lead-free ferroelectric materials. However, barium titanate ceramics has low dielectric constant at room temperature, so doping is an effective method to tailor its performance [4-6]. Much research has proved that Zr is a very suitable substitute in BT to form Ba(Ti<sub>1-x</sub>Zr<sub>x</sub>)O<sub>3</sub> (BZT) solid solution, the substitute of Zr in barium titanate ceramics can not only to shift the  $T_c$  to lower temperature, but also to broaden the temperature dependence of dielectric constant [7-9]. Indeed, when  $x \geq 0.25$ , BaZr<sub>x</sub>Ti<sub>1-x</sub>O<sub>3</sub> (BZT) system shows a relaxor state, which has been rooted from a breakage in the correlation displacement of B-site cations caused by

---

\* Corresponding author: miles-li@qq.com

the substitution of  $\text{Ti}^{4+}$  by  $\text{Zr}^{4+}$  [10-12]. Lualhe' et al. [12] found that the local structure around Zr differs considerably from the average cubic structure investigated by X-ray diffraction and the distance between Zr atoms and their first oxygen neighbors is equal to the distance measured in the  $\text{BaZrO}_3$  compound independently of the Zr substitution rate. The authors observed that Zr atoms tended to be segregated in Zr-rich regions and the relaxor behavior in BZT could be influenced by the random elastic fields generated by the chemical arrangement of Zr atoms.

Combined with previous studies, the BZT ceramics has high dielectric properties at room temperature. The effect of various dopants such as  $\text{Ce}^{4+}$ ,  $\text{Y}^{3+}$ ,  $\text{Ho}^{3+}$  and  $\text{Ca}^{2+}$  on a BZT system has been studied [13–16]. In order to further improve the dielectric properties, the effects of the content and sintering temperature on the crystal structure, microstructure and dielectric properties of  $\text{BaZr}_{0.1}\text{Ti}_{0.9}\text{O}_3$  (BZT10) base ceramics were studied by adding  $\text{Gd}_2\text{O}_3$ .

## 2. Experimental

The general formula of the materials studied was  $\text{BaZr}_{0.1}\text{Ti}_{0.9}\text{O}_3 + x \text{Gd}_2\text{O}_3$ , where  $x=0.0-0.7$  mol%. The samples were prepared by the two-stage method to acquire a pure phase of perovskite. Reagent-grade oxide powders,  $\text{TiO}_2$ ,  $\text{BaCO}_3$ ,  $\text{ZrO}_2$  and  $\text{Gd}_2\text{O}_3$ , were used as the starting materials. At first, a powder of  $\text{BaZr}_{0.1}\text{Ti}_{0.9}\text{O}_3$ , was prepared by calcination of  $\text{BaCO}_3$ ,  $\text{TiO}_2$  and  $\text{ZrO}_2$ , at  $1100^\circ\text{C}$  for 2 h. Secondly, the above precursor with  $\text{Gd}_2\text{O}_3$  was weighed and mixed through use of a polyethylene jar and agate balls milling media. The mixture was then dried at  $120^\circ\text{C}$ , granulated (with polyvinyl alcohol as binder), pressed into the desired form ( $\Phi \times d = 12.30 \times 2.00 \text{ mm}^2$ ) at 160 Mpa, and then sintered at  $1280^\circ\text{C}$ ,  $1300^\circ\text{C}$ ,  $1330^\circ\text{C}$  and  $1350^\circ\text{C}$  for 2 h in the air, respectively. The obtained samples were cleaned by an ultrasonic bath, and then dried. Both sides of the obtained samples were screened electrode paste, and then fired at  $610^\circ\text{C}$  for 10 minutes.

The crystal feature of the samples was analyzed by X-ray diffractometer (XRD, Model RIGAKU D/MAX 2500V/PC, Japan) with a  $2\theta$  range from  $10^\circ$  to  $70^\circ$ . The surface micrographs of the samples were observed by field emission scanning electron microscopy (SEM, Hitachi s4800). The temperature dependence of the dielectric constant ( $\epsilon$ ) and the dielectric loss ( $\tan\delta$ ) was measured using a capacitance apparatus (Model YY 281 automatic LCR Meter 4225) at 1 kHz in a temperature range over  $0^\circ\text{C}$  to  $130^\circ\text{C}$ .

## 3. Results and discussions

The XRD patterns of the samples with different amounts of  $\text{Gd}_2\text{O}_3$  contents sintered at  $1350^\circ\text{C}$  for 2 h are shown in Fig. 1. It can be seen from Fig. 1 that after doping with different amounts of  $\text{Gd}_2\text{O}_3$ ,  $\text{Ba}(\text{Zr}_{0.1}\text{Ti}_{0.9})\text{O}_3$  ceramics all have characteristic peaks of perovskite structure, and  $\text{Gd}_2\text{O}_3$  with different doping quantities does not cause too many changes in the structure of BZT crystals. Therefore, it can be inferred that the  $\text{Ba}(\text{Zr}_{0.1}\text{Ti}_{0.9})\text{O}_3 + x \text{Gd}_2\text{O}_3$  ceramic is a tetragonal phase at room temperature, and the amount of doping does not change the main crystal phase structure of the  $\text{Ba}(\text{Zr}_{0.1}\text{Ti}_{0.9})\text{O}_3$  ceramics.

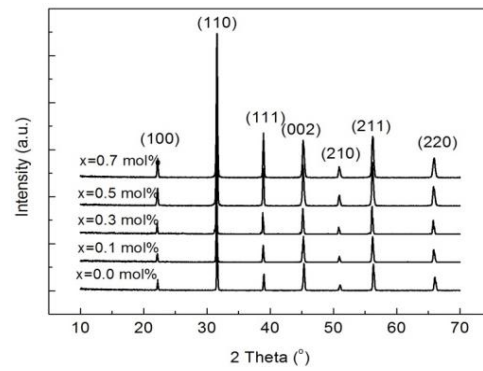


Fig. 1. XRD patterns of the  $Gd_2O_3$  doped BZT10 ceramics.

Fig. 2 shows the SEM images of  $Gd^{3+}$ -doped BZT10 ceramics. As can be seen from Fig. 2, the grain boundaries for different  $Gd_2O_3$  doped  $Ba(Zr_{0.1}Ti_{0.9})O_3$  ceramic are relatively clear. The crystal size of pure barium zirconate titanate ceramics is uneven and the density is small.

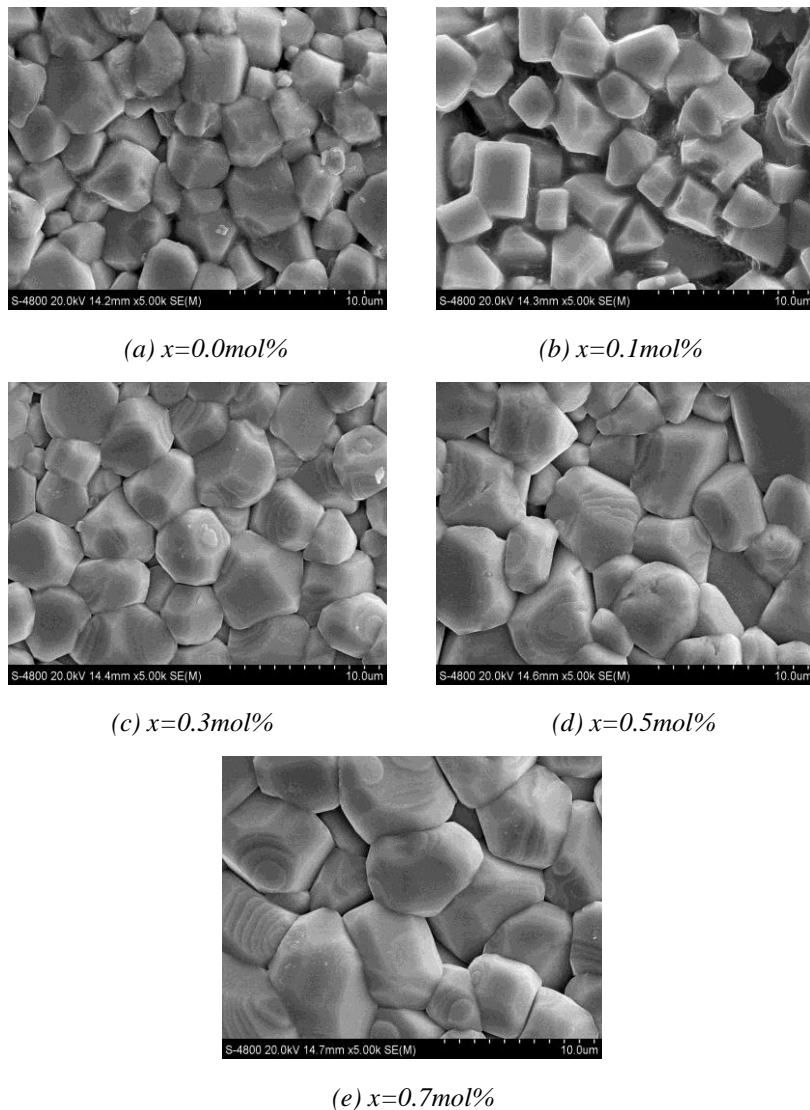


Fig. 2. Surface SEM images of the  $Gd_2O_3$  doped BZT10 ceramics.

A small amount of  $Gd_2O_3$  doped sample grain presents a regular boundary. The size of the grain is slightly smaller, and the liquid phase is produced, resulting in an increase in density. With the increase of  $Gd_2O_3$  content, the grain size increases continuously, and its shape is ellipsoidal, and the porosity increases and the density decreases. When the doping amount  $x \geq 0.5$  mol%, the grain size basically remains unchanged, the grain size is uniform, and the density increases. The result is also consistent with the following analysis of dielectric properties at room temperature because the porosity of the ceramic body has a great influence on the dielectric properties of dielectric ceramics.

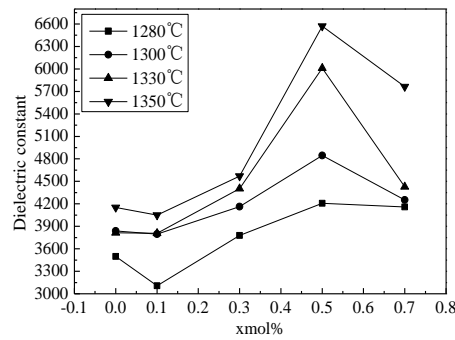


Fig. 3. Dielectric constant of BZT10 ceramics with various  $Gd_2O_3$  doping concentration.

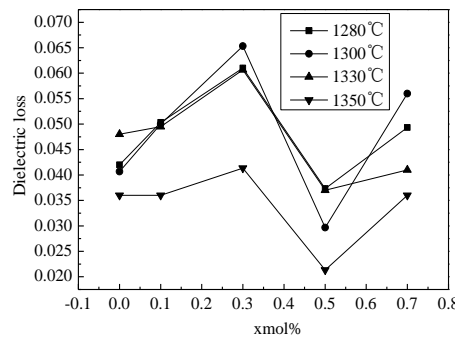


Fig. 4. Dielectric loss of BZT10 ceramics with various  $Gd_2O_3$  doping concentration.

Fig. 3 and Fig. 4 show influence of  $Gd^{3+}$  content on dielectric constants and dielectric loss of the samples sintered at 1280 °C, 1300 °C, 1330 °C and 1350 °C for 2 h, respectively.

As can be seen from Fig. 3 and Fig. 4, with the  $Gd_2O_3$  content increasing, the dielectric constants rose first and then decreased under different sintering conditions of 1280 °C, 1300 °C, 1330 °C, and 1350 °C. When the sintering temperature is 1350 °C and the  $Gd^{3+}$  doping amount is  $x = 0.5$  mol%, the dielectric loss is minimal, the dielectric constant is the highest, and the dielectric performance at room temperature is optimal.

In the initial stage, the dielectric constant increases with the increase of the doping  $Gd^{3+}$  concentration. On the one hand,  $Gd^{3+}$  enters the A site, since the radius of  $Gd^{3+}$  is smaller than that of  $Ba^{2+}$ , the cell parameter decreases, causing the lattice to shrink, then the lattice distortion increases, accordingly the spontaneous polarization of the crystal increases, so the dielectric constant of the ceramic sample increases. On the other hand, when  $Gd^{3+}$  enters the A site, the electron can be generated, the appearance of these electrons will increase the electron conductivity

of the sample, and the weak bound electrons are easy to interact with the positive charge at A site, therefore, the electron polarization and ion polarization of the crystal are weakened, and the dielectric constant of the ceramic sample is increased. When  $x(\text{Gd}_2\text{O}_3) > 0.3$  mol%,  $\text{Gd}^{3+}$  will partially enter the B site, resulting in a part of the oxygen vacancy. Due to the nail action of the oxygen vacancy, the sample dielectric constant will be reduced, and the oxygen vacancy can inhibit  $\text{Ti}^{4+}$  to  $\text{Ti}^{3+}$  reduction, resulting in the reduce of dielectric loss [17].

At the sintering temperature of 1350 °C for 2 h, the curves of dielectric constants and dielectric loss with temperature are shown in Fig. 5 and Fig. 6 for different  $\text{Gd}_2\text{O}_3$  doped BZT ceramics. It can be seen from the figure that when  $x(\text{Gd}_2\text{O}_3) = 0.5$  mol%, the maximum dielectric peak of the sample is highest. From the previous analysis, at this time,  $\text{Gd}^{3+}$  enters the A site, and the cell parameter decreases, resulting in a contraction of the lattice of the sample and a large lattice distortion, then the polarization ability is enhanced. Therefore, the ferroelectricity of the sample increases, and the dielectric constant at the Curie point increases. When  $x(\text{Gd}_2\text{O}_3) > 0.5$  mol%, the Curie dielectric peak of the specimen is suppressed, the dielectric peak becomes significantly wider, and the specimen becomes relatively flat near the Curie dielectric peak, which is obviously related to the electrons generated by  $\text{Gd}^{3+}$  entering the B site. The dielectric loss of different  $\text{Gd}_2\text{O}_3$  doped samples showed an overall trend of decreasing with temperature change. When the doping of  $\text{Gd}_2\text{O}_3$  was 0.5 mol%, the dielectric loss of the sample was minimized and remained at about 0.015.  $\text{Gd}_2\text{O}_3$  doping has little effect on the movement of the Curie point of BZT ceramics, and the Curie temperature is about 60 °C, but the doping of  $\text{Gd}_2\text{O}_3$  can increase the peak of the dielectric peak at the Curie point.

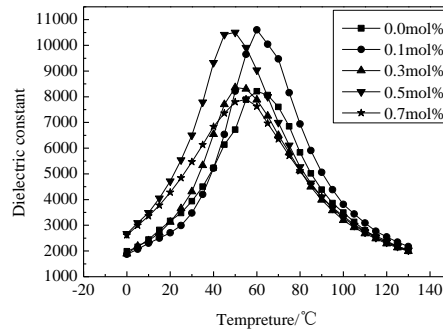


Fig. 5. Temperature dependence of dielectric constant of  $\text{Gd}_2\text{O}_3$  doped BZT10 ceramics.

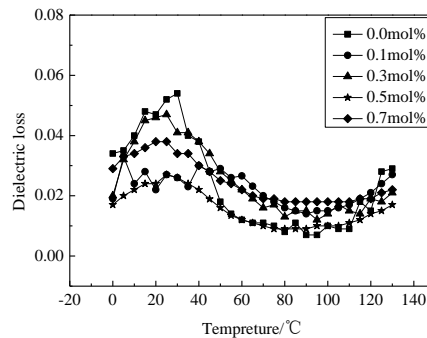


Fig. 6. Temperature dependence of dielectric loss of  $\text{Gd}_2\text{O}_3$  doped BZT10 ceramics.

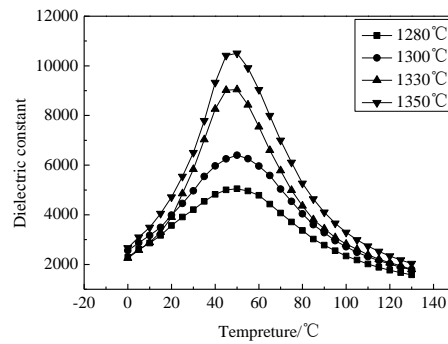


Fig. 7. Temperature dependence of dielectric constant of 0.5 mol%  $Gd_2O_3$  doped BZT10 ceramics at various sintering temperature.

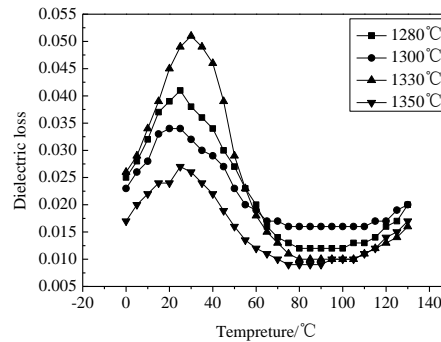


Fig. 8. Temperature dependence of dielectric loss of 0.5 mol%  $Gd_2O_3$  doped BZT10 ceramics at various sintering temperature.

Fig. 7 and Fig. 8 show the variation of dielectric constant and dielectric loss with temperature at different sintering temperatures for 0.5 mol%  $Gd_2O_3$  doped BZT10 ceramics. It can be seen from the figure that with the increase of sintering temperature, the dielectric constant increases and the dielectric loss decreases. The increase of sintering temperature can increase the dielectric constant at Curie temperature and reduce the dielectric loss, and this is mainly related to the fact that the grain development is more complete, the material becomes more dense, and the porosity decreases with the increase of sintering temperature.

#### 4. Conclusions

The BZT10 ceramics are prepared using solid state reaction method. Effects of  $Gd_2O_3$  dopant on microstructure and dielectric properties of BZT10 ceramics are investigated. The crystal structure for  $Gd_2O_3$  doped  $Ba(Zr_{0.1}Ti_{0.9})O_3$  ceramics is a single perovskite structure, and the doping of  $Gd^{3+}$  does not generate new phase. Owing to the dopant of  $Gd^{3+}$ , the grain size increases continuously at first with the  $Gd_2O_3$  concentration increasing, when the doping amount  $x \geq 0.5$  mol %, the grain size basically remains unchanged, the grain size is uniform. In the initial stage,  $Gd^{3+}$  ion enters the A site, the cell parameter decreases, accordingly the spontaneous polarization

of the crystal increases, so the dielectric constant of the ceramic sample increases. When  $x(\text{Gd}_2\text{O}_3) > 0.3$  mol %,  $\text{Gd}^{3+}$  can partially enter the B site, generating the oxygen vacancy. Due to the action of the oxygen vacancy, the sample dielectric constant will be reduced, and the oxygen vacancy can inhibit  $\text{Ti}^{4+}$  to  $\text{Ti}^{3+}$  reduction, resulting in the reduce of dielectric loss. Thanks to the dopant of  $\text{Gd}^{3+}$ , the dielectric loss is minimal, the dielectric constant is the highest, and the dielectric performance at room temperature is optimal when the sintering temperature is 1350 °C and the  $\text{Gd}^{3+}$  doping amount is  $x = 0.5$  mol %.

### Acknowledgements

This work is partially supported by Shijiazhuang University Teaching Reform Research Project (2016) and the Scientific Research Projects of Colleges and Universities in Hebei Province (Grant No. Z2014112), P. R. China.

### References

- [1] X. W. Jiang, H. Hao, S. J. Zhang, J. H. Lv, M. H. Cao, Z. H. Yao, H. X. Liu, *Journal of the European Ceramic Society* **39**(4), 1103(2019).
- [2] W. J. Chen, H. Hao, Y. Yang, C. Chen, M. Appiah, Z. H. Yao, M. H. Cao, Z. Y. Yu, H. X. Liu, *Ceramics International* **43**(11), 8449(2017)
- [3] S. M. Olhero, A. Kaushal, J. M. F. Ferreira, *Journal of the European Ceramic Society* **35**(9), 2471(2015).
- [4] U. Obilor, C. Pascual-Gonzalez, S. Murakami, L. M. Reaney, A. Feteira, *Materials Research Bulletin* **97**, 385(2018).
- [5] Z. Rashad, A. Feteira, *Materials Letters* **222**, 180(2018).
- [6] D. Xu, W. L. Li, L. D. Wang, W. P. Cao, W. D. Fei, *Acta Materialia* **79**, 84(2014).
- [7] M. Shen, W. R. Li, M. Y. Li, H. Liu, J. M. Xu, S. Y. Qiu, G. Z. Zhang, Z. X. Lu, H. L. Li, S. L. Jiang, *Journal of the European Ceramic Society* **39**(5), 1810(2019).
- [8] Y. L. Li, R. R. Wang, X. G. Ma, Z. Q. Li, R. L. Sang, Y. F. Qu, *Materials Research Bulletin* **49**, 601(2014).
- [9] Y. L. Li, W. X. Dun, S. H. Yan, G. F. Zuo, Y. F. Qu, Z. Q. Li, *Journal of Materials Science: Materials in Electronics* **28**(16), 11636(2017).
- [10] V. V. Shvartsman, D. C. Lupascu, *Journal of the American Ceramic Society* **95**, 1(2012).
- [11] C. Laulhe, F. Hippert, J. Kreisel, M. Maglione, A. Simon, J. L. Hazemann, V. Nassif, *Physical Review B* **74**(1), 014106(2006).
- [12] C. Laulhe', F. Hippert, R. Bellissent, A. Simon, G. J. Cuello, *Physical Review B* **79**(6), 064104 (2009).
- [13] Y. R. Cui, X. Y. Liu, M. H. Jiang, X. Y. Zhao, X. Shan, W. H. Li, C. H. Yuan, C. R. Zhou, *Ceramics International* **38**(6), 4761(2012).
- [14] W. Li, J. G. Hao, W. F. Bai, Z. J. Xu, R. Q. Chu, J. W. Zhai, *Journal of Alloys and Compounds* **531**(5), 46(2012).

- [15] W. Li, Z. J. Xu, R. Q. Chu, P. Fu, P. An, *Ceramics International* **38**(5), 4353(2012).
- [16] S. K. Ye, J. Fuh, L. Lu, *Journal of Alloys and Compounds* **541**(15), 396(2012).
- [17] B. Su, T. W. Button, *Journal of Applied Physics* **95**(3), 1382 (2004).